

# Site-specific translocation and evidence of postnatal origin of the t(1;19) *E2A-PBX1* fusion in childhood acute lymphoblastic leukemia

Joseph L. Wiemels<sup>\*†</sup>, Brian C. Leonard<sup>\*</sup>, Yunxia Wang<sup>‡</sup>, Mark R. Segal<sup>\*</sup>, Stephen P. Hunger<sup>§</sup>, Martyn T. Smith<sup>‡</sup>, Vonda Crouse<sup>¶</sup>, Xiaomei Ma<sup>‡</sup>, Patricia A. Buffler<sup>‡</sup>, and Sharon R. Pine<sup>||</sup>

<sup>\*</sup>Department of Epidemiology and Biostatistics, University of California, San Francisco, CA 94143; <sup>†</sup>School of Public Health, University of California, Berkeley, CA 94720; <sup>‡</sup>Department of Pediatrics, University of Florida College of Medicine, Gainesville, FL 32611; <sup>§</sup>Valley Children's Hospital, 9300 Valley Children's Place, FC13, Madera, CA 93638; and <sup>¶</sup>Children's Cancer Research Laboratory, Basic Science Building Room 401, New York Medical College, Valhalla, NY 10595

Edited by Janet D. Rowley, University of Chicago Medical Center, Chicago, IL, and approved September 10, 2002 (received for review August 9, 2002)

The t(1;19) translocation yields a fusion between *E2A* and *PBX1* genes and occurs in 5% of acute lymphoblastic leukemia in children and adults. We used chromosomal translocations and Ig heavy chain (*IGH*)/T cell antigen receptor (*TCR*) rearrangements to develop an understanding of the etiology and natural history of this subtype of leukemia. We sequenced the genomic fusion between *E2A* and *PBX1* in 22 preB acute lymphoblastic leukemias and two cell lines. The prenatal origin of the leukemia was assessed in 15 pediatric patients by screening for the clonotypic *E2A-PBX1* translocation in neonatal blood spots, or Guthrie cards, obtained from the children at the time of birth. Two patients were determined to be weakly positive for the fusion at the time of birth, in contrast to previously studied childhood leukemia fusions, t(12;21), t(8;21), and t(4;11), which were predominantly prenatal. The presence of extensive *N*-nucleotides at the point of fusion in the *E2A-PBX1* translocation as well as specific characteristics of the *IGH/TCR* rearrangements provided additional evidence for a postnatal, preB cell origin. Intriguingly, 16 of 24 breakpoints on the 3.2-kb *E2A* intron 14 were located within 5 bp, providing evidence for a site-specific recombination mechanism. Breakpoints on the 232-kb *PBX1* intron 1 were more dispersed but highly clustered proximal to exon 2. In sum, the translocation breakpoints displayed evidence of unique temporal, ontological, and mechanistic formation than the previously analyzed pediatric leukemia translocation breakpoints and emphasize the need to differentiate cytogenetic and molecular subgroups for studies of leukemia causality.

Pediatric leukemias are a group of diverse diseases at the chromosome level, with various subtypes recognizable by recurrent translocations and aneuploidies. Although these genetic abnormalities help to categorize leukemias for treatment strategy and prognosis, they also may delineate specific causal pathways to malignancy. The consideration of individual molecular subtypes is providing clarity to epidemiological and biological studies. The best characterized example of this approach is the infant leukemias with *MLL* translocations (*MLL*<sup>+</sup>), for which epidemiologic associations and molecular analysis of breakpoints point to an *in utero* origin of the translocations, with reactive metabolites of genotoxic chemicals playing a potential key role (1–5). The *MLL*<sup>+</sup> leukemias, along with the hyperdiploid subtype (leukemia clones with >50 chromosomes), also display significant associations with variants in genes encoding functional metabolic enzymes, thus implying a risk of leukemia imparted by the enzymes' substrates or products (6–8). Childhood leukemias with *TEL-AML1* translocations, representing ≈25% of common acute lymphoblastic leukemia (cALL), share the *in utero* timing of translocation formation with *MLL*<sup>+</sup> leukemias (9); however, there is currently no etiological mechanism for the formation of this translocation, apart from the nonhomologous end-joining processes that rejoin broken DNA.

The second most common translocation in acute lymphoblastic leukemia (ALL) is t(1;19), which fuses the 5' end of *E2A* with most of *PBX1*, yielding a chimeric protein that has cell transformation capability in both *in vitro* and *in vivo* models (reviewed in ref. 10). This leukemia subtype is morphologically and prognostically distinct in origin from the cALL subtype and represents ≈25% of the preB cell (CD10<sup>+</sup>, CD19<sup>+</sup>, CD34<sup>-</sup>, cIgμ<sup>+</sup>, sIgμ<sup>-</sup>) leukemia and 5% of childhood and adult ALL overall (11). The leukemia is a well established clinical and biologic entity, reinforced by its unique transcriptome (12); however, the timing, origin, and mechanism of the genetic rearrangements that create this leukemia are unclear. Like most B cell origin leukemias, *E2A-PBX1* leukemias have germline-rearranged Ig heavy chain (*IGH*) rearrangements (13). The combinatorial and diversity characteristics in the leukemic *IGH* CDR3 region have been used to signify early (prenatal) from later (postnatal) development of normal lymphocytes as well as various pediatric leukemia subtypes (14–16). To date, no examples of the *E2A-PBX1* translocation have been sequenced at the genomic level, nor has the natural history of this subtype been explored.

We developed methods to sequence *E2A-PBX1* fusions rapidly at the genomic DNA level and have assessed whether this fusion arose prenatally by using archived neonatal blood spots, or Guthrie cards. Translocation breakpoints displayed a high degree of clustering and clear evidence of the involvement of a site-specific recombination mechanism. Little evidence for prenatal origin was found by direct assessment of the Guthrie spots, and indirect evidence from *IGH* and T cell antigen receptor (*TCR*) rearrangement patterns supported a postnatal origin with ontological specificity.

## Materials and Methods

**Cell Lines and Patient Samples.** Cell lines were obtained from American Type Culture Collection (cell line RCH-ACV) and cell line 697 was kindly provided by Michael Cleary (Stanford University, Stanford, CA). Patient samples were derived from the Northern California Childhood Leukemia study (#69, 71, 131, 348, 416, 398, and 498). Additional samples came from the Children's Oncology Group ALL cell bank (#058, 062, 228, 295, 482, 513, 633, 777, 780, and 913) and patients treated at University of Colorado Health Sciences Center (D1, D2, D3, and D4) or Stanford Medical Center (S1). Guthrie cards were obtained from the Genetic Diseases Branch of the California Department of Health Services.

This paper was submitted directly (Track II) to the PNAS office.

Abbreviations: ALL, acute lymphoblastic leukemia; *IGH*, Ig heavy chain; R55, recombinase site sequences.

<sup>†</sup>To whom correspondence should be addressed at: Laboratory for Molecular Epidemiology, Department of Epidemiology and Biostatistics and Comprehensive Cancer Center, University of California, Box 0560, San Francisco, CA 94143. E-mail: wiemels@itsa.ucsf.edu.

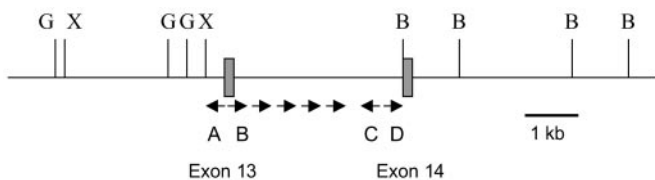


**Fig. 1.** Inverse PCR scheme. Locations of PCR primers and restriction sites around intron 13 of the *E2A* gene. G, *Bgl*II; X, *Xba*I; B, *Bam*HI; A, location of *invA* and *invA*-1 primers; B, location of *invB* and *invB*-1 primers. *InvB*-2, 3, 4, and 5 are located just to the right of *invB*-1. C corresponds to *invC* and *invC*-1; D corresponds to *invD* and *invD*-1, respectively. *InvC*-2, 3, 4, and 5 are the complement of *invB*-5, 4, 3, and 2, respectively.

**Translocation Sequencing.** *E2A-PBX1* fusions were sequenced by using Long Distance Inverse PCR (LDI-PCR) as described (17) with modifications. LDI-PCR was performed from the *E2A* sequence, given that the breakpoint cluster region is only 3.2 kb. The enzymes *Bgl*II and *Xba*I permitted amplification of *E2A-PBX1* sequences, whereas enzymes *Bam*HI, *Hpa*I, and *Bsr*DI were used to amplify the reciprocal *PBX1-E2A* (Fig. 1). PCRs were nested, using primers *E2A* A and B for the first round and *E2A* A-1 and B-1 for the second round, for amplifying *E2A-PBX1* fusions. For the reciprocal translocation, C and D primers were used in turn (Fig. 1, and see primers in Table 2, which is published as supporting information on the PNAS web site, www.pnas.org). A rearrangement would be predicted to introduce a restriction site on the opposite side of the intron, allowing the preferential amplification of a smaller rearranged band over the larger wild type. After an initial successful nested PCR, tertiary reactions were performed by using *E2A* A-1 in all tubes with, in separate tubes, B-2, B-3, B-4, and B-5.

Guthrie card screening, or “backtracking,” was carried out by using Ampdirect methods, as described (9, 18), with two modifications. First, the presoaking in distilled water was omitted. Second, both primary and secondary reactions were performed by using Ampdirect buffers. The primary round was a 50- $\mu$ l reaction with 1/16 segment of a 1.5-cm<sup>2</sup> Guthrie card. The second round was a 25- $\mu$ l reaction using 1  $\mu$ l of the first round for template. The soaking step was omitted based on the observation that Guthrie cards stored in the freezer (as all California cards are) tend to leach DNA during this procedure. Primer sequences and product sizes can be found in Table 3, which is published as supporting information on the PNAS web site.

**IGH/TCR Rearrangement Analysis.** *IGH* CDR3 region and *TCR $\delta$*  gene rearrangements were amplified by PCR as described (19). PCR products were separated on a 6% polyacrylamide gel and scanned and analyzed with a FluorImager 595 laser scanner and IMAGEQUANT software (Amersham Pharmacia). Clonal rearrangements were directly sequenced from agarose gel-purified PCR products as described (19).

Sequences were analyzed for *V<sub>H</sub>*, *D<sub>H</sub>*, and *J<sub>H</sub>* segments by using MACVECTOR 7.0 (Genetics Computer Group, Madison, WI). For *D<sub>H</sub>* identification (20), the criteria of a minimum of either seven uninterrupted *D<sub>H</sub>* germline nucleotides, or at least eight *D<sub>H</sub>* germline nucleotides with no more than one mismatch and at least two matching nucleotides at both the 5' and 3' ends, were used (21). No *DIR* segments, inverted *D* segments, or *D-D* recombinations were accepted (20).

**Statistical Analysis.** Translocation breakpoint clustering was assessed by using a scan statistic as described (22). Prediction of heptamer-nonamer V(D)J recombinase site sequences (RSS; CACAGTG, 12 or 23 nucleotides, ACAAAACC) was assessed by using the following rubric: the underlined sequence must be

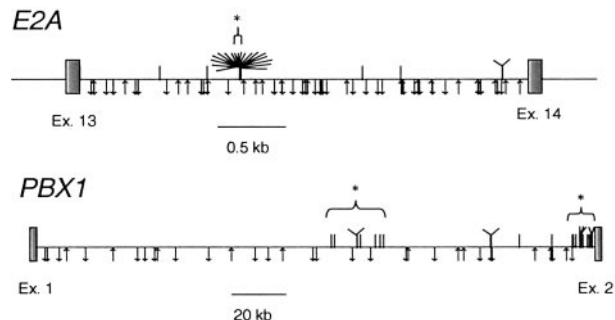


**Fig. 2.** Locations of *E2A-PBX1* breakpoints and V(D)J recombinase sites. Exon sequences are indicated with boxes, and intronic sequences are indicated with horizontal lines. Patient breakpoints are identified with hash marks above the introns, and putative cryptic RSS are indicated below the introns. V(D)J sites are shown with an up arrow if they are on the sense strand and a down arrow if antisense. Eighteen breakpoints within a 12-bp segment of *E2A* are shown as a tree-like structure, and brackets above the introns (with a \*) show the clusters indicated in Results.

present, but any other nucleotide was allowable as long as there were less than 10 (*E2A*) or 5 (*PBX*) mismatches. A more stringent definition of RSS was chosen for the *PBX1* gene because of the fact that the intron is much larger, although RSS distribution was similar regardless of stringency (data not shown). Both forward and complement sequences were scanned for RSS.

## Results

***E2A-PBX1* Genomic Fusions.** Sequences were obtained for 24 available patient or cell-line DNAs for *E2A-PBX1*. Sixteen breakpoints were located within 5 bp on the *E2A* side and two others within 12 bp, whereas breakpoints were more widely spaced on the *PBX1* introns (Fig. 2). Overall assessment for clustering was highly significant on both introns. The single cluster of 18 breakpoints spanning 12 bp on *E2A* (see Figs. 2 and 3) signified a cluster by scan statistic ( $P < 0.0001$ ), whereas two clusters were evident on *PBX1*: one proximal to exon 2 (12 breakpoints within 8,137 bp,  $P < 0.0001$ ) and one in the right center of the intron (8 breakpoints within 21,400 bp,  $P = 0.056$ ). A single base of *E2A* at which six *E2A-PBX1* translocations were placed was also the site for two previously sequenced *E2A-HLF* and one base pair away from another *E2A-HLF* (Fig. 3; refs. 23 and 24). The *PBX1* clusters were much more dispersed but still statistically clustered because of the lengthy intronic region of *PBX1*.

Upon LDI-PCR and sequencing analysis, two unrelated patients (#69 and 131) exhibited the same *E2A-PBX1* fusion

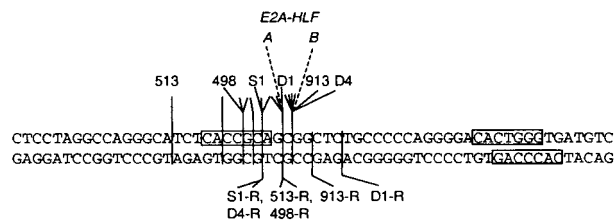


**Fig. 3.** Fine structure of cluster region on *E2A*. Eighteen forward *E2A-PBX1* breakpoints are indicated with lines and labels above the sequence segment of *E2A* intron 13, and six reciprocal (i.e., *PBX1-E2A*) breakpoints are indicated below the segment. The vertical lines delimit the *E2A* sequence to the left of the line for the *E2A-PBX1* and delimit the *E2A* sequence to the right of the line in the case of the reciprocal. Six *E2A-PBX1* translocations are designated at a single base, at which two *E2A* breakpoints from previously sequenced *E2A-HLF*<sup>+</sup> patients were located, as shown with a dashed line (B, ref. 23). An additional *E2A-HLF* breakpoint is located 1 bp prior to A (24). Candidate RSS heptamers are boxed; nonamers are not shown for clarity.

**Table 1. Age, gender, and genomic rearrangements in t(1;19) E2A-PBX1 patients**

Patient ID	Age, yr.mo	Gender	N-Nucl.* E2A-PBX1	IGH #	N-Nucl. IGH	Frame <sup>†</sup> IGH	Vδ2-Dδ3 #	N-Nucl. Vδ2-Dδ3
398	1.8	F	13	1	28	I	0	
913	1.8	M	41 (0)	1	9	I	0	
482	2.3	F	7	1	6	O	0	
777	2.5	M	6	1	19	I	0	
697	4	F	1	1	34	S	1	8
348	4.3	M	13	1	39	I	0	
131	4.4	M	2	0			2	3
228	4.8	M	-1	1	4	I	0	
633	5.1	F	6	1	13	I	0	
295	5.3	F	4	1	14	I	0	
780	6.6	F	18	1	14	I	1	8
69	6.9	F	2	1	13	I	0	
498	7.3	F	15 (9)	1	17	I	1	10
513	7.6	F	4 (15)	1	17	I	0	
RCH	8	F	14	1	16	O	1	9
71	8.2	F	2	1	27	I	1	14
58	8.7	F	11	1	21	I	1	7
D1	9.5	F	15 (5)	1	14	I	1	6
D2	10.2	F	16	0			1	
416	11.2	F	19	1	14	I	1	3
62	12.5	F	17	1	22	I	0	
D3	17.6	M	39	1	17	I	1	7
D4	47.11	F	9 (6)	1	15	I	0	
S1	NA <sup>‡</sup>	NA	15 (16)	1	25	S	0	

\*N-Nucl. are nontemplate nucleotides. N-nucleotides for reciprocal fusions are in parentheses.

<sup>†</sup>Pertains to IGH rearrangements. I, in frame and functional; O, out of frame and nonfunctional; S, in frame but stop codon.

<sup>‡</sup>NA, not available.

sequence, including the presence of two nontemplate nucleotides “TT” at the point of fusion. To assess whether laboratory contamination may have played a role, we sequenced the IGH and TCR rearrangements of the patients as well as five polymorphisms that were found to be different (Table 1, supporting information, and data not shown). The breakpoints were confirmed by using a second diagnostic sample. The two patients were diagnosed at the same hospital, but because diagnosis and sample processing took place 18 months apart, it is unlikely that contamination was introduced within the laboratory or the hospital.

Twenty-three of 24 breakpoints (96%) contained the presence of 1–41 N-nucleotides. These are nontemplate nucleotides not present in either parent DNA sequence but probably introduced through the activity of terminal deoxynucleotidyltransferase (TdT) before ligation of DNA ends (Fig. 4). Only a single breakpoint did not contain N-nucleotides but displayed microhomology of one nucleotide at the fusion junction (#228). Another breakpoint exhibited a 30-bp duplication of PBX1 intronic sequence at the breakpoint along with 5 and 14 N-nucleotides at the E2A and PBX1 sides of the duplication, respectively (RCH-ACV, Fig. 4). Sequencing of reciprocal fusions (the 5' end of the PBX1 gene fused to the 3' end of E2A) was attempted in all cases but was successful in only five patients (Figs. 3 and 4). The rate of success (5 of 24 patients = 21%) is not far from the rate at which molecular and cytogenetically reciprocal translocations are identifiable in t(1;19)<sup>+</sup> leukemia (25%; ref. 25). An additional patient exhibited a fusion between the intron 13 of E2A and intron 2 of the RODH 3-hydroxysteroid epimerase gene on chromosome 12 (#513, Fig. 4). The predicted fusion protein would not be in the proper reading frame but would result in the 3' ends of each gene fused back-to-back, with no promoter (data not shown). Overall, when compared with other pediatric leukemia translocations, the reciprocal fusions

were very conservative, demonstrating breakpoints in close proximity (average = 5 bp, excluding one with a 1-bp microhomology) to the primary fusion and also harboring similar presence of N-nucleotides.

Tight clustering of the breakpoints along E2A, along with the presence of N-nucleotides, suggests the activity of the V(D)J recombinase. Such a mechanism has one additional requirement: the presence of a canonical RSS consisting of a heptamer-nonamer sequence near the junction. This sequence would by rule be positioned in an orientation that would result in its excision from the E2A gene, because the N-nucleotides are added to the coding joint (26). Functional studies have identified basic requirements of functional RSS (CACAGTG, 12 or 23 nucleotides, ACAAAAACC), with the underlined nucleotides being present in close to 100% of functional RSS (27, 28). Breakpoints using the RSS yield a perfectly conserved pair of signal sequences linked to each other in reverse orientation and a modified coding end sequence which often has nucleotide loss (“nibbling”) as well as nucleotide gain (N-nucleotides) that contribute to the variable region of the IGH or TCR (reviewed in ref. 26). The slightly variable (within five nucleotides) nature of the E2A cluster as well as the presence of the N-nucleotides suggests that it may serve as a surrogate coding end in an aberrant V(D)J mechanism. However, the reciprocal fusions did not display signal end-like fusions, which typically consists of two abutting signal sequences with the lack of N-nucleotides, but instead showed similar characteristics of the forward fusion. We searched for potentially cryptic V(D)J RSS within the E2A and PBX1 introns and found no exact matches but many near matches that could conceivably serve as weak RSS and contribute to the translocation (28–30). In general, there were no apparent relationships between the locations of breakpoints and the generally even spreading of putative cryptic RSS sequences along the intronic regions (Fig. 2). Of course, this analysis does not take

Pt.	<i>E2A</i>	<i>N</i>	<i>PBX1</i>
416	TGGAGCAGAGTAAGGAGAGG	ttaatgggtaacttttcgg	TTTGTGAAAGCATTGTAGAA
633	GGATTTCTGGCCCGAGCTGT	aggtctc	CCCACCCCTACCCACACATTC
777	ATCACTCTTAGGCCAGGGCA	aactga	CCTACAAATAGGTGAAAGTT
513	TCTAGGCCAGGGCATCTCA	tcca	GGCTCTGTCAACTGTGTA
513 (R)	TCCCCTGGGGCAGAGCCGC	ctcacegcacettta	AGCATGCTGTTGGGTAGAAG
482	CTAAGCCAGGGCATCTCACC	eggetct	AATTCCTCATTTCTCTCTTT
131/69	CTAAGCCAGGGCATCTCACC	tt	CCCATCCAGAAAGCCAGGGC
498	TAGGCCAGGGCATCTCACC	ggttcggtctcgggg	CTAACCATGATGGTGGAAAGA
498 (R)	GGCATTCTATCACCAATA	aagaagggc	GGGCTCTGCCCCACAGGGAC
398	TTGCCAGGGCATCTCACC	caccaaatcaaaa	TACCCCTCTCTGGTTATAAT
780	AGGCCAGGGCATCTCACC	cgcatctgatccggtgcgc	ATATGTGATGACGCTCAAA
81	AGGCCAGGGCATCTCACC	tgacttggctcgctcg	AAGAGGATACCCCTGAGCTC
81 (R)	ACATCACCCAGNCTCCCTG	gggttgggctcgctct	GGGCNCCTTTTCTGTATAT
058	GCCAGGGCATCTCACC	tgggttcagcg	GAGCTGGCTGGAGCATAGG
D1	GCCAGGGCATCTCACC	agaagggaacatccc	GTTTCTCTCTCTCAGCTCAG
D1 (R)	CCGAGTGTCCCTGGGGGCA	gggt	TTTCTTAAGAGCAATATAATA
D3	GCCAGGGCATCTCACC	Gaaccgacgcaactaagcgaacccctcgaaatttcgga	LTTCACAGCTTTCCACAGGC
913	CAGGGCATCTCACC	Gcccaagggttaaggccttcctatgaaagagcgcacacaa	AGACTAGTAGTATTTTA
913 (R)	CGTCCCTGGGGCAGAGC		<i>TGZTCCAATCTCGAGAAA</i>
697	CCAGGGCATCTCACC	t	TGCTTTATGCTTTTAGCTTT
348	CCAGGGCATCTCACC	acgcccgaatat	CATGGCTTAGGAGAACCGTG
71	CCAGGGCATCTCACC	ag	CANGTGAGGGCGGAGTTGC
D2	CCAGGGCATCTCACC	aaggagggttgggtcc	GCTGGGCCCTGCTGCCAGAT
D4	CCAGGGCATCTCACC	tggagtcgg	CAGACATTTAGTGTCCAGGG
D4 (R)	GCTGGGGCAGAGCCGCTG	tcgccc	AGATAAAGAACAGACAGAA
RCH-ACV	ATCTCTTATGATGCTGAAGC	agccc gggccaagaatccc	GCTGTGGCTAACGCTGCTCTCAGCTGAA GACAAAGGATCTGGGATCT
62	TGTTTTTTTGGAGACAGG	ccccctactgaaccctc	CBAAGGAAAGAGGGTCCAGA
228	CCCTTTTCATCTTGTGTCT	T	CTTGAATGCTGGGATTA
295	TTGATCTGTGTCTTAAAT	ggccc	ATTTTCTCATTGCAAGTT
478	CTAAGCCAGGGCATCTCACC	cggtcct	ATTCTAATTTTCTCATTT

**Fig. 4.** Fine structure of *E2A-PBX1* genomic fusions. Patient number is displayed with the *E2A* and *PBX1* sequences proximal to the fusions and *N*-nucleotides that were present between the *E2A* and *PBX1* sequence (lowercase letters). The antisense strand of the reciprocal fusions (R) are displayed. Cell line RCH had two segments of *N*-nucleotides along with a tandem duplication of 30 nucleotides of *PBX1* sequences shown in between, derived from sequence 7,398 bp 3' of the breakpoint in reverse orientation. The "T" is a microhomology nucleotide (derived from *E2A* or *PBX1*, not an *N*-nucleotide). The reciprocal partner fusion to 913 is in italics, indicating a fusion of *E2A* to *RODH* intron 2.

into account other aspects of DNA or chromatin structure that could influence accessibility of the DNA to recombinase activating *RAG* proteins. Some potential RSS in vicinity of the *E2A* cluster were found (Fig. 3). However, the closest putative RSS is in the orientation such that the *E2A* breakpoint in the *E2A-PBX1* translocation would be the "coding end" fusion. If this were the case, the breakpoints should be oriented to the left side of the closest putative RSS sequence (Fig. 3), however 17 of 18 breakpoints are on the right side of the "CAC." By these criteria there is poor evidence to support V(D)J-RSS to account for the breakpoint cluster on *E2A*. The *PBX1* translocations were not site-specific, nor did they have potential V(D)J RSS at breakpoint fusions, and, thus, displayed little evidence of RSS-mediated recombination. However, the breakpoints were highly clustered at the 3' end of the 232-kb intron 2 of this gene (Fig. 2).

**Backtracking *E2A-PBX1* to Birth.** Fifteen patients were assessed for prenatal origin of the clonotypic *E2A-PBX1* translocation by PCR amplification of Guthrie cards from those individuals. Sensitivities of PCR reactions were initially determined by using a dilution series of patient diagnostic DNA that was derived from blood or bone marrow at the time of diagnosis, and each assay was run with the dilution series to assess sensitivity, which ranged from 5 to 500 pg. For each patient, a total of 12 segments (3/4

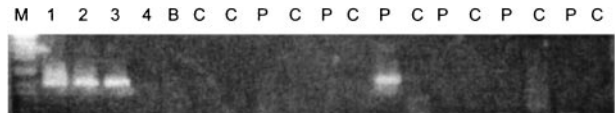


**Fig. 5.** Guthrie card analysis of patient #295. The second-round PCR products are shown for the dilution series of diagnostic patient DNA (lanes 1–4, 1:10 dilution series, starting at 50 ng/ $\mu$ l patient DNA in lane 1). Guthrie card segments for control (C) cards are shown with segments from patient #295 (P) and a no-DNA blank (B). A single-lane positive shown was sequenced and determined to match the sequence from the patient. Results were similar for patient #58.

of one spot) were assayed in two PCR reactions (6 per reaction). Only one segment each from two patients (58 and 295) were identified to be "positive" for prenatal origin, indicated by the presence of leukemia clone-specific DNA sequence within the Guthrie segment in one assay (Fig. 5). This positive assay was not repeated in the second assessment of six segments for these patients. Sensitivity for patient #295 was 500 pg of DNA and 5 pg for patient #58. We cannot rule out lack of PCR sensitivity or lack of circulating *E2A-PBX1* cells as a reason for the negative results in the other 13 cases; therefore, we recognize that those assays are indeterminate for prenatal origin of the clone.

**IGH and TCR Rearrangements.** The leukemic cells from 24 t(1;19) positive ALL patients were analyzed for clonal rearrangements of the *IGH* and *TCR* genes. Every patient was positive for at least one clonal rearrangement. One patient was positive for two V $\delta$ 2-D $\delta$ 3, and nine were positive for 1 *IGH* and 1 V $\delta$ 2-D $\delta$ 3 rearrangements. No clonal D $\delta$ 2-D $\delta$ 3 rearrangements were identified. Of the 22 *IGH* rearrangements identified, 20 were "in frame"; i.e., the triplet codon structure was maintained through the rearrangement. However, stop codons were introduced within two of these as a result of the rearrangement. Therefore, 18 of 22 (82%) would be predicted to translate into functional *IGH* heavy chains (Table 1 and Table 4, which is published as supporting information on the PNAS web site).

In normal *IGH* rearrangements, J<sub>H4</sub> is the most commonly used J<sub>H</sub> segment at all stages of development, and J<sub>H2</sub>, J<sub>H3</sub>, and J<sub>H6</sub> are the next most common J<sub>H</sub> segments during first trimester, third trimester, and adults, respectively (21). In our study, J<sub>H4</sub> and J<sub>H6</sub> were used in equal frequency (7/22 = 32% each), followed by J<sub>H5</sub> (5/22) and J<sub>H1</sub>, J<sub>H2</sub>, and J<sub>H3</sub> (one of each, see supporting information). Members of the D<sub>H3</sub> family are normally observed in a higher percentage of *IGH* rearrangements as the age of the study population increases. For example, 5% of first trimester, 10% of second trimester, and 33% of adult sequences harbor D<sub>H3</sub> segments (21). In our study, 9 of the 27 D<sub>H</sub> gene segments were identified in the clonal *IGH* rearrangements of the ALL patients. The D<sub>H3</sub> family was represented most frequently (45%). The D7–27 gene segment is represented in 33% of fetal marrow B-lineage cells, in 17% of preterm infant mature B cells, and only in 1–2% of the adult D<sub>H</sub> segments (21, 31, 32). We observed no D7–27 segments in the 22 *IGH* rearrangements examined. In sum, the usages of J<sub>H</sub> and D<sub>H</sub> are consistent with a postnatal chronological age at which the blood cells that exhibit the leukemic phenotype passed through the developmental stage in which *IGH* rearrangement occurred.

The frequency of the V $\delta$ 2-D $\delta$ 3 rearrangement in childhood preB ALL reaches 32–35% (13, 33), and its presence is correlated with age; i.e., 86% of those younger than 2, 43% of those from 2 to 14, and 18% of those older than 15 were positive for V $\delta$ 2-D $\delta$ 3 (13). We identified V $\delta$ 2-D $\delta$ 3 rearrangements in 46% of the patients in our study, but identified no significant correlation between age and the presence of V $\delta$ 2-D $\delta$ 3 rearrangements ( $P > 0.9$ , Pearson's correlation). The frequency of the D $\delta$ 2-D $\delta$ 3

rearrangement in childhood preB ALL is historically  $\approx 13\%$  (34). We found no clonal D $\delta 2$ -D $\delta 3$  rearrangements in the 24 t(1;19)<sup>+</sup> patients in our study. A lower-than-expected frequency in our population may be because of a small sample size.

**IGH N-Nucleotides.** The developmental regulation of nongermline (*N*) region addition has been well documented (21, 32, 35, 36). D<sub>H</sub>J<sub>H</sub> joining that lack *N* regions are found more frequently at the fetal stage of development. The proportion of sequences containing *N* additions increases from 25% during the second trimester to 94% in adults (21). In our study, all 22 clonal *IGH* gene rearrangements contained *N*-nucleotides (100%). The mean lengths of the *N*-regions on the 5' and 3' sides of the DH region were 10.4 and 7.3 nucleotides, respectively. The *N*-region lengths are consistent with those observed in adults, which average 8 and 6 nucleotides, respectively (32). There was no relationship between *N*-nucleotides at any of the three types of rearrangements assayed (i.e., *IGH*, *TCRD*, or *E2A-PBX1*; *P* > 0.4) and age at diagnosis.

## Discussion

Childhood leukemia predominantly originates from B cell precursors, which are characterized by rapid developmental stage-specific proliferation as well as the activation of the V(D)J recombinase system. V(D)J and switch recombinases are the only mechanism in the body targeted to the somatic rearrangement of the genome and are well known to be involved in some translocation fusion breakpoints in another B cell cancer, the lymphomas (reviewed in ref. 37). It is reasonable to suppose that translocations in the B cell leukemias might arise from the aberrant activity of V(D)J recombinase; however, recent studies have failed to substantiate this hypothesis and, instead, suggest the activity of topoisomerase II, *Alu*-mediated homologous recombination, or unspecified damage-repair mechanisms involving DNA double-strand break repair without the involvement of recombinase-associated RSS sequences (38–40). This fact holds true for the most frequent translocation subtype of childhood ALL, *TEL-AML1* fusions, which are generally widely spread over intron 5 of *TEL* and introns 1–2 of *AML1*. There is evidence of clustering of these breakpoints, but such clustering is multifocal and dispersed with cluster widths of hundreds of nucleotides rather than relegated to specific well defined recombination sites typical of V(D)J recombinase-induced genomic rearrangements (22, 41).

In contrast to other childhood leukemia breakpoints, *E2A* breakpoints were clustered in a site-specific manner. Sixteen *E2A-PBX1* translocations of 24 were clustered within 5 bp (see *Results*). Three reported fusions between *E2A* and *HLF* also had breakpoints within the same cluster (Fig. 3; refs. 23 and 24). This clustering is the type evident in normal *IGH* and *TCR* V(D)J recombination, as well as putative V(D)J recombination events in other genes such as *HPRT* (42) and also in T cell oncogenic mutations at the *TAL* and *MTS1* loci (43, 44) but not at any other B cell leukemia-associated breakpoints. The clustering exhibited on the *E2A* side thus suggests the involvement of the site-specific V(D)J recombinase. Indeed, the *E2A* gene itself produces the E12/E47 proteins that function as indispensable transcription factors for the induction of V(D)J recombination (45, 46), indicating that the chromatin configuration of the *E2A* gene itself is likely to be in an open conformation because of the fact that it is being transcribed, thus potentially accessible to recombinases. The ontological point at which *E2A-PBX1* translocation occurs is likely to be later than that of other pediatric leukemia translocations that do not demonstrate site-specific clustering or the presence of extensive *N*-nucleotides. However, as explained in *Results*, there is no recombinase site sequence in the *E2A* gene in the correct orientation to account for typical V(D)J mechanisms. Although the presence of *N*-nucleotides clearly indicates

the expression of TdT during the translocation process, further research will have to define the nature of the site-specific recombination and whether alternate mechanisms, such as transposase activity of *RAG* genes, might play a role in the mechanism of *E2A-PBX1*.

Breakpoints in the far larger exon 2 of *PBX1* were clustered in a more dispersed manner compared with *E2A*. DNA breaks on the *PBX1* side may be caused by factors in common with those inducing other pediatric chromosomal translocations, which are similarly clustered on a diffuse scale; for instance, *TEL-AML1*, *AML1-ETO*, and *MLL-AF4* (38, 39, 41). DNA double-strand breaks induced by means other than *RAG*-induced recognition may be competent to participate in ligation to the *E2A* breakpoint. Interestingly, most *PBX1* translocations were crowded next to exon 2, which suggests a contribution from chromatin, gene structure, or perhaps the presence of an open locus control region near the exon. The final ligation step between *E2A* and *PBX1* is likely to be a nonhomologous end-joining event, in common with other translocations, as there is no evidence of homologous recombination.

The presence of nontemplate *N*-nucleotides at *E2A-PBX1* fusions stands in marked contrast to the dearth of such nucleotides at *TEL-AML1* fusions. It is known that normal V(D)J junctions formed during fetal development usually lack, or contain very few, *N*-nucleotides, whereas fusions in children and adults usually contain these nucleotides (21, 32, 35, 36). The lack of such nucleotides in *TEL-AML1* fusions, and more importantly, the demonstration that clonotypic fusions present in leukemia cells at the time of diagnosis are present in the Guthrie cards of the children who later got disease (9), argues for the prenatal origin of these fusions. The presence of *N*-nucleotides at *E2A-PBX1* fusions and *IGH* rearrangements as well as the J<sub>H</sub> and D<sub>H</sub> segment usage (see *Results*) does not date the timing of the fusion but supports a postnatal fusion event at a later ontological stage of blood cell development. In addition, the Guthrie card study did not support a prenatal origin for *E2A-PBX1* translocations in the majority of cases, providing weak evidence in two. PCR analysis of clonotypic *IGH* sequences on Guthrie cards was not performed because of the limitations in the resource in relationship to the scientific value derived from backtracking *IGH* sequences.

Lymphomas are B cell tumors that are also caused, at least in part, by translocations that result in dysregulated gene expression. The mechanisms involved in forming these oncogenic translocations have been linked to the *IGH* rearrangement processes that occur at the same maturation stage exhibited by the lymphoma (37, 47–49). Also, the normal antibody-producing *IGH* rearrangements in the lymphomas (not involved in oncogenic translocation) display characteristics typical of the phenotype of normal B cells from the organ from which the lymphoma is derived, providing evidence that the timing of transformation is linked in developmental stage with normal function of these B cells (reviewed in ref. 50). Pediatric leukemias, on the other hand, may harbor translocation before the cell-specific developmental stage at which the leukemia phenotype is clinically observed, given the lack of V(D)J evidence at translocation fusions despite rearranged *IGH* genes within the leukemia clones (15, 17, 51). In addition, the *IGH* genes are nonfunctional (i.e., out of frame) two thirds of the time in B cell leukemias, indicating that *IGH* rearrangement occurs without selection processes (15). This fact, along with the fact that B cell leukemias often include additional *IGH* subclones as well as cross-lineage *TCR* rearrangements (52), provides evidence that the transforming event for the cell precedes *IGH* rearrangement, because normal selection processes would result in deletion of these clones or further V(D)J recombination to produce a functional *IGH* gene. The exception to this could be t(1;19) *E2A-PBX1*<sup>+</sup> leukemia, which may be derived from a preB cell transformation,

post-*IGH* rearrangement, because 82% of the 22 rearranged *IGH* genes studied here are predicted to produce functional, in-frame genes (Table 1). This characteristic would argue that the t(1;19) *E2A-PBX1* translocation as a transformation event occurred at the same time as or after *IGH* rearrangement and subsequent selection, linking transformation with the ontological stage of the leukemic cell. In addition, the pattern of germline segment usage and junctional diversity of the t(1;19)<sup>+</sup> patients is consistent with rearranged *IGH* chain variable regions and *TCR* rearrangements typically seen in adults but rare during fetal development. In sum, these data suggest a more lymphoma-like etiology for t(1;19)<sup>+</sup> leukemia than the other pediatric leukemias.

We conclude that the preB cells undergoing leukemic transformation that result in t(1;19)<sup>+</sup> ALL typically undertake translocation as well as *IGH* gene rearrangement after birth in ontologically more mature cells than those involved in the majority of pediatric lymphocytic leukemias. Combined with its

status as a unique clinical entity, t(1;19)<sup>+</sup> ALL is a distinct subtype that should be stratified separately in etiology studies. The molecular analysis and natural history of gene rearrangements provide additional confidence in our strategy of stratification of this and other molecularly defined leukemia subtypes in the study of the causes of childhood leukemia.

We thank Andrew Carroll for cytogenetic analysis of COG patients and Cheryl Willman for maintenance of COG specimens. We thank Luoping Zhang and Weihong Guo (University of California, Berkeley), and ChangHong Yin and Qianxu Guo (New York Medical College) for technical assistance. We also thank Peggy Reynolds, Fred Lorey, and Michael Layefsky for coordinating Guthrie card retrieval, Institutional Review Board approval, and data management between the Children's Oncology Group and the California Department of Health Services. This work was supported by National Institutes of Health Grants CA89032 (to J.L.W.), ES09137, ES04705, and ES01896 (to M.T.S. and P.A.B.), Children's Oncology Group Grant CA30969, and the Children's Cancer Fund (to S.R.P.).

- Strick, R., Strissel, P. L., Borgers, S., Smith, S. L. & Rowley, J. D. (2000) *Proc. Natl. Acad. Sci. USA* **97**, 4790–4795.
- Alexander, F. E., Patheal, S. L., Biondi, A., Brandalise, S., Cabrera, M. E., Chan, L. C., Chen, Z., Cimino, G., Cordoba, J. C., Gu, L. J., et al. (2001) *Cancer Res.* **61**, 2542–2546.
- Ford, A. M., Ridge, S. A., Cabrera, M. E., Mahmoud, H., Steel, C. M., Chan, L. C. & Greaves, M. (1993) *Nature* **363**, 358–360.
- Gale, K. B., Ford, A. M., Repp, R., Borkhardt, A., Keller, C., Eden, O. B. & Greaves, M. F. (1997) *Proc. Natl. Acad. Sci. USA* **94**, 13950–13954.
- Ross, J. A., Potter, J. D., Reaman, G. H., Pendergrass, T. W. & Robison, L. L. (1996) *Cancer Causes Control* **7**, 581–590.
- Wiemels, J. L., Pagnamenta, A., Taylor, G. M., Eden, O. B., Alexander, F. E. & Greaves, M. F. (1999) *Cancer Res.* **59**, 4095–4099.
- Wiemels, J. L., Smith, R. N., Taylor, G. M., Eden, O. B., Alexander, F. E. & Greaves, M. F. (2001) *Proc. Natl. Acad. Sci. USA* **98**, 4004–4009.
- Smith, M. T., Wang, Y., Skibola, C. F., Slater, D., Lo Nigro, L., Nowell, P. C., Lange, B. J. & Felix, C. A. (2002) *Blood*, in press.
- Wiemels, J. L., Cazzaniga, G., Daniotti, M., Eden, O. B., Addison, G. M., Maser, G., Saha, V., Biondi, A. & Greaves, M. F. (1999) *Lancet* **354**, 1499–1503.
- Aspland, S. E., Bendall, H. H. & Murre, C. (2001) *Oncogene* **20**, 5708–5717.
- Borowitz, M. J., Hunger, S. P., Carroll, A. J., Shuster, J. J., Pullen, D. J., Steuber, C. P. & Cleary, M. L. (1993) *Blood* **82**, 1086–1091.
- Yeoh, E. J., Ross, M. E., Shurtleff, S. A., Williams, W. K., Patel, D., Mahfouz, R., Behm, F. G., Raimondi, S. C., Relling, M. V., Patel, A., et al. (2002) *Cancer Cells* **1**, 133–143.
- Brumpt, C., Delabesse, E., Beldjord, K., Davi, F., Cayuela, J. M., Millien, C., Villaresse, P., Quartier, P., Buzyn, A., Valensi, F. & Macintyre, E. (2000) *Blood* **96**, 2254–2261.
- Wasserman, R., Galili, N., Ito, Y., Reichard, B. A., Shane, S. & Rovera, G. (1992) *J. Exp. Med.* **176**, 1577–1581.
- Steenbergen, E. J., Verhagen, O. J., van Leeuwen, E. F., Behrendt, H., Merle, P. A., Wester, M. R., von dem Borne, A. E. & van der Schoot, C. E. (1994) *Eur. J. Immunol.* **24**, 900–908.
- Fasching, K., Panzer, S., Haas, O. A., Borkhardt, A., Marschalek, R., Griesinger, F. & Panzer-Grumayer, E. R. (2001) *Blood* **98**, 2272–2274.
- Wiemels, J. L. & Greaves, M. (1999) *Cancer Res.* **59**, 4075–4082.
- Wiemels, J. L., Xiao, Z., Boffler, P. A., Maia, A. T., Ma, X., Dicks, B. M., Smith, M. T., Zhang, L., Feusner, J., Wiencke, J., et al. (2002) *Blood* **99**, 3801–3805.
- Mayer, S., Giamelli, J., Sandoval, C., Roach, A., Ozkaynak, M. F., Tugal, O., Rovera, G. & Jayabose, S. (1999) *Leukemia* **13**, 1843–1852.
- Corbett, S. J., Tomlinson, I. M., Sonnhammer, E. L., Buck, D. & Winter, G. (1997) *J. Mol. Biol.* **270**, 587–597.
- Shiohara, S., Mortari, F., Lima, J. O., Nunez, C., Bertrand, F. E., III, Kirkham, P. M., Zhu, S., Dasanayake, A. P. & Schroeder, H. W., Jr. (1999) *J. Immunol.* **162**, 6060–6070.
- Segal, M. R. & Wiemels, J. L. (2002) *J. Am. Stat. Assoc.* **97**, 66–76.
- Inaba, T., Roberts, W. M., Shapiro, L. H., Jolly, K. W., Raimondi, S. C., Smith, S. D. & Look, A. T. (1992) *Science* **257**, 531–534.
- Hunger, S. P., Ohyashiki, K., Toyama, K. & Cleary, M. L. (1992) *Genes Dev.* **6**, 1608–1620.
- van Dongen, J. J., Macintyre, E. A., Gabert, J. A., Delabesse, E., Rossi, V., Saglio, G., Gottardi, E., Rambaldi, A., Dotti, G., Griesinger, F., et al. (1999) *Leukemia* **13**, 1901–1928.
- Lewis, S. M. (1994) *Adv. Immunol.* **56**, 27–150.
- Hesse, J. E., Lieber, M. R., Mizuuchi, K. & Gellert, M. (1989) *Genes Dev.* **3**, 1053–1061.
- Lewis, S. M., Agard, E., Suh, S. & Czyzyk, L. (1997) *Mol. Cell. Biol.* **17**, 3125–3136.
- Raghavan, S. C., Kirsch, I. R. & Lieber, M. R. (2001) *J. Biol. Chem.* **276**, 29126–29133.
- Marculescu, R., Le, T., Simon, P., Jaeger, U. & Nadel, B. (2002) *J. Exp. Med.* **195**, 85–98.
- Yamada, M., Wasserman, R., Reichard, B. A., Shane, S., Caton, A. J. & Rovera, G. (1991) *J. Exp. Med.* **173**, 395–407.
- Zemlin, M., Bauer, K., Hummel, M., Pfeiffer, S., Devers, S., Zemlin, C., Stein, H. & Versmold, H. T. (2001) *Blood* **97**, 1511–1513.
- Breit, T. M., Wolvers-Tettero, I. L., Hahlen, K., van Wering, E. R. & van Dongen, J. J. (1991) *Leukemia* **5**, 1076–1086.
- Seriu, T., Erz, D., Stark, Y. & Bartram, C. R. (1997) *Leukemia* **11**, 759–761.
- Gu, H., Forster, I. & Rajewsky, K. (1990) *EMBO J.* **9**, 2133–2140.
- Sanz, I. (1991) *J. Immunol.* **147**, 1720–1729.
- Kuppers, R. & Dalla-Favera, R. (2001) *Oncogene* **20**, 5580–5594.
- Reichel, M., Gillert, E., Angermuller, S., Hensel, J. P., Heidel, F., Lode, M., Leis, T., Biondi, A., Haas, O. A., Strehl, S., et al. (2001) *Oncogene* **20**, 2900–2907.
- Xiao, Z., Greaves, M. F., Boffler, P. A., Smith, M. T., Segal, M. R., Dicks, B. M., Wiencke, J. K. & Wiemels, J. L. (2001) *Leukemia* **15**, 1906–1913.
- Atlas, M., Head, D., Behm, F., Schmidt, E., Zeleznik-Le, N. H., Roe, B. A., Burian, D. & Domer, P. H. (1998) *Leukemia* **12**, 1895–1902.
- Wiemels, J. L., Alexander, F. E., Cazzaniga, G., Biondi, A., Mayer, S. P. & Greaves, M. (2000) *Genes Chromosomes Cancer* **29**, 219–228.
- Fuscoe, J. C., Zimmerman, L. J., Lippert, M. J., Nicklas, J. A., O'Neill, J. P. & Albertini, R. J. (1991) *Cancer Res.* **51**, 6001–6005.
- Breit, T. M., Beishuizen, A., Ludwig, W. D., Mol, E. J., Adriaansen, H. J., van Wering, E. R. & van Dongen, J. J. (1993) *Leukemia* **7**, 2004–2011.
- Cayuela, J. M., Gardie, B. & Sigaux, F. (1997) *Blood* **90**, 3720–3726.
- Romanow, W. J., Langerak, A. W., Goebel, P., Wolvers-Tettero, I. L., van Dongen, J. J., Feeney, A. J. & Murre, C. (2000) *Mol. Cell* **5**, 343–353.
- Goebel, P., Janney, N., Valenzuela, J. R., Romanow, W. J., Murre, C. & Feeney, A. J. (2001) *J. Exp. Med.* **194**, 645–656.
- Marculescu, R., Le, T., Bocskor, S., Mitterbauer, G., Chott, A., Mannhalter, C., Jaeger, U. & Nadel, B. (2002) *Leukemia* **16**, 120–126.
- Nadel, B., Marculescu, R., Le, T., Rudnicki, M., Bocskor, S. & Jager, U. (2001) *Leuk. Lymphoma* **42**, 1181–1194.
- Welzel, N., Le, T., Marculescu, R., Mitterbauer, G., Chott, A., Pott, C., Kneba, M., Du, M. Q., Kusec, R., Drach, J., et al. (2001) *Cancer Res.* **61**, 1629–1636.
- Hummel, M. & Stein, H. (2000) *Curr. Opin. Oncol.* **12**, 395–402.
- Reichel, M., Gillert, E., Nilson, I., Siegler, G., Greil, J., Fey, G. H. & Marschalek, R. (1998) *Oncogene* **17**, 3035–3044.
- Szczepanski, T., Beishuizen, A., Pongers-Willems, M. J., Hahlen, K., Van Wering, E. R., Wijkhuijs, A. J., Tibbe, G. J., De Bruijn, M. A. & Van Dongen, J. J. (1999) *Leukemia* **13**, 196–205.